AMERICAN SOCIETY FOR MICROBIOLOGY | Journal of Bacteriology®

RESEARCH ARTICLE

Interaction between *Streptococcus pneumoniae* and *Staphylococcus aureus* Generates ·OH Radicals That Rapidly Kill *Staphylococcus aureus* Strains

Xueqing Wu,[a,f] Oren Gordon,[g] Wenxin Jiang,[a] Brenda S. Antezana,[b] Uriel A. Angulo-Zamudio,[h] Carlos del Rio,[a] Abraham Moller,[b] Terry Brissac,[i] Aimee R. P. Tierney,[b] Kurt Warncke,[e] Carlos J. Orihuela,[i] Timothy D. Read,[b,c,d] Jorge E. Vidal[a,b,c*]

[a]Hubert Department of Global Health, Rollins School of Public Health, Emory University, Atlanta, Georgia, USA
[b]Graduate Program in Microbiology and Molecular Genetics, Emory University, Atlanta, Georgia, USA
[c]Antibiotic Research Center, Emory University, Atlanta, Georgia, USA
[d]School of Medicine, Emory University, Atlanta, Georgia, USA
[e]Department of Physics, Emory University, Atlanta, Georgia, USA
[f]Department of Infectious Disease, Sir Run Run Shaw Hospital, College of Medicine, Zhejiang University, Hangzhou, China
[g]Department of Pediatrics, Hadassah-Hebrew University Medical Center, Jerusalem, Israel
[h]Regional Program for the Doctorate in Biotechnology, Faculty of Chemical Sciences Biological, Autonomous University of Sinaloa, Sinaloa, Mexico
[i]Department of Microbiology, University of Alabama at Birmingham, Birmingham, Alabama, USA

ABSTRACT *Streptococcus pneumoniae* rapidly kills *Staphylococcus aureus* by producing membrane-permeable hydrogen peroxide (H_2O_2). The mechanism by which *S. pneumoniae*-produced H_2O_2 mediates *S. aureus* killing was investigated. An *in vitro* model that mimicked *S. pneumoniae*-*S. aureus* contact during colonization of the nasopharynx demonstrated that *S. aureus* killing required outcompeting densities of *S. pneumoniae*. Compared to the wild-type strain, isogenic *S. pneumoniae* Δ*lctO* and *S. pneumoniae* Δ*spxB*, both deficient in production of H_2O_2, required increased density to kill *S. aureus*. While residual H_2O_2 activity produced by single mutants was sufficient to eradicate *S. aureus*, an *S. pneumoniae* Δ*spxB* Δ*lctO* double mutant was unable to kill *S. aureus*. A collection of 20 diverse methicillin-resistant *S. aureus* (MRSA) and methicillin-susceptible *S. aureus* (MSSA) strains showed linear sensitivity (R^2 = 0.95) for *S. pneumoniae* killing, but the same strains had different susceptibilities when challenged with pure H_2O_2 (5 mM). There was no association between the *S. aureus* clonal complex and sensitivity to either *S. pneumoniae* or H_2O_2. To kill *S. aureus*, *S. pneumoniae* produced ~180 μM H_2O_2 within 4 h of incubation, while the killing-defective *S. pneumoniae* Δ*spxB* and *S. pneumoniae* Δ*spxB* Δ*lctO* mutants produced undetectable levels. Remarkably, a sublethal dose (1 mM) of pure H_2O_2 incubated with *S. pneumoniae* Δ*spxB* eradicated diverse *S. aureus* strains, suggesting that *S. pneumoniae* bacteria may facilitate conversion of H_2O_2 to a hydroxyl radical (·OH). Accordingly, *S. aureus* killing was completely blocked by incubation with scavengers of ·OH radicals, dimethyl sulfoxide (Me_2SO), thiourea, or sodium salicylate. The ·OH was detected in *S. pneumoniae* cells by spin trapping and electron paramagnetic resonance. Therefore, *S. pneumoniae* produces H_2O_2, which is rapidly converted to a more potent oxidant, hydroxyl radicals, to rapidly intoxicate *S. aureus* strains.

IMPORTANCE *Streptococcus pneumoniae* strains produce hydrogen peroxide (H_2O_2) to kill bacteria in the upper airways, including pathogenic *Staphylococcus aureus* strains. The targets of *S. pneumoniae*-produced H_2O_2 have not been discovered, in part because of a lack of knowledge about the underlying molecular mechanism. We demonstrated that an increased density of *S. pneumoniae* kills *S. aureus* by means of H_2O_2 produced by two enzymes, SpxB and LctO. We discovered that SpxB/

Citation Wu X, Gordon O, Jiang W, Antezana BS, Angulo-Zamudio UA, del Rio C, Moller A, Brissac T, Tierney ARP, Warncke K, Orihuela CJ, Read TD, Vidal JE. 2019. Interaction between *Streptococcus pneumoniae* and *Staphylococcus aureus* generates ·OH radicals that rapidly kill *Staphylococcus aureus* strains. J Bacteriol 201:e00474-19. https://doi.org/10.1128/JB.00474-19.

Editor Michael J. Federle, University of Illinois at Chicago

Address correspondence to Jorge E. Vidal, jvidal@umc.edu.

* Present address: Jorge E. Vidal, Department of Microbiology and Immunology, University of Mississippi Medical Center, Jackson, Mississippi, USA.

X.W., O.G., and W.J. contributed equally to this work.

Received 17 July 2019
Accepted 8 August 2019
Accepted manuscript posted online 12 August 2019
Published 4 October 2019

LctO-produced H_2O_2 is converted into a hydroxyl radical (·OH) that rapidly intoxicates and kills *S. aureus*. We successfully inhibited the toxicity of ·OH with three different scavengers and detected ·OH in the supernatant. The target(s) of the hydroxyl radicals represents a new alternative for the development of antimicrobials against *S. aureus* infections.

KEYWORDS *Staphylococcus aureus*, *Streptococcus pneumoniae*, eradication, hydrogen peroxide, hydroxyl radicals

Streptococcus pneumoniae and *Staphylococcus aureus* colonize the upper airways of humans, forming persistent biofilms (1–9). Once in the nasopharynx, *S. pneumoniae* forms a biofilm that increases resistance to desiccation and antibiotic resistance and also provides a source of planktonic bacteria that migrate to the ears, lower respiratory tract, circulation, heart, and meninges, causing pneumococcal disease, the burden of which is extremely high in the human population (5, 6, 10–13). *S. aureus* strains colonize the skin of >30% of the human population but also reside in the nasopharynx, causing severe pathologies, including bacteremia and pneumonia (1, 3, 7, 11, 14, 15).

Over the last few years, our laboratories and others have conducted carriage studies of important human pathogens in the nasopharynxes of children of different ethnicities. These studies demonstrated a negative association for the concurrent carriage of *S. pneumoniae* and *S. aureus* (3, 7, 16). Soon after pneumococcal conjugate vaccines (PCV) became available, a potential mechanistic competition between *S. pneumoniae* and *S. aureus* for the colonization of the upper airways was observed. Some of the first studies showed that nasopharyngeal carriage of *S. aureus* increased in children who had received PCV. The increased *S. aureus* colonization was attributed to the decreased carriage of pneumococcal serotypes targeted by PCV (1, 7, 8). It is therefore clear that *S. pneumoniae in vivo* interferes with colonization by *S. aureus*.

Although evidence that *S. pneumoniae* was capable of killing *S. aureus* was published over 100 years ago (17, 18), studies of the molecular mechanism(s) behind these epidemiological observations were reinitiated when the pneumococcal vaccine was licensed in early 2000 in developed countries. Pericone et al. (19), and then other investigators, demonstrated that pneumococcal strains isolated from disease or carriage interfered with the growth of *S. aureus* in broth cultures. The proposed mechanism involved the production of hydrogen peroxide (H_2O_2) that was released by *S. pneumoniae* into the supernatant (20). This H_2O_2-mediated killing of *S. aureus* occurred within 6 h post-inoculation of *S. pneumoniae*, but it was inhibited in cocultures with catalase added; by incubating these cocultures in an anaerobic chamber; or by a mutation within the *spxB* gene, encoding the enzyme streptococcal pyruvate oxidase, which endogenously produces H_2O_2 during conversion of acetylphosphate from pyruvate (19–23). Notably, SpxB accounts for ~85% of the membrane-permeable H_2O_2 that is released by the bacteria into the supernatant (24, 25). A second contributor to the pool of H_2O_2 released by bacteria is the enzyme lactate dehydrogenase (LctO), which converts lactate to pyruvate (24, 26). While the mechanism by which *S. pneumoniae* kills *S. aureus* strains has been related to production of H_2O_2, only *spxB* mutants have been assessed (20, 27).

SpxB-produced H_2O_2 has also been involved in inducing cytotoxicity to lung cells, apoptosis, and the toxic events observed when *S. pneumoniae* invades the central nervous system and heart, albeit the specific mechanism(s) mediating this damage is still to be clarified (12, 13). Moreover, *S. pneumoniae* mutants in the *spxB* gene produced less capsule, due to the lack of acetylated capsule precursors, and were attenuated for virulence in mouse models of pneumococcal disease (25, 28). The attenuated virulence phenotype can be explained in part by a recent publication showing that endogenously produced H_2O_2 was required to release the toxin pneumolysin (29).

In contrast to the *in vitro* evidence presented above, studies conducted using an animal model of colonization demonstrated that *S. aureus* colonized the nasal cavity of neonatal rats even when it was inoculated concurrently with *S. pneumoniae* strain

TIGR4 or with an H_2O_2-deficient TIGR4 Δ*spxB* mutant (30). When the TIGR4 wild type (wt) or an isogenic TIGR4 Δ*spxB* mutant was inoculated along with *S. aureus* in animals, *S. aureus* colonization densities were similar whether *S. pneumoniae* produced hydrogen peroxide or not (30, 31). Therefore, the role of *S. pneumoniae*-produced H_2O_2 in interfering with *S. aureus* growth has been debated (32). Killing of *S. aureus* by incubation with pure H_2O_2, however, has already been documented (33, 34). A dose of ~10 mM H_2O_2 was required to kill *S. aureus* bacteria (19), whereas preloading *S. aureus* with iron reduced the bactericidal dose to ~1 mM (33, 34). The presence of intracellular iron was required to generate, by the Fenton reaction, the hydroxyl radical (·OH) (34), which is a stronger oxidant than H_2O_2 itself (35). Other bacterial species are also susceptible to H_2O_2 at a concentration similar to that killing *S. aureus*, with ~2.5 mM H_2O_2 showing the maximal killing rate for *Escherichia coli* (35–37).

We recently demonstrated that the *S. pneumoniae*-induced killing of *S. aureus* biofilms, including those formed by methicillin-resistant *S. aureus* (MRSA) strains, was enhanced by physical contact (23). Complete eradication of ~10^9 *S. aureus* bacteria within *S. pneumoniae*-*S. aureus* biofilms occurred within 4 h of incubation. Furthermore, washed *S. pneumoniae* bacteria were more lethal to *S. aureus* strains than their H_2O_2-containing supernatants, suggesting pneumococcal cells may be required to convert H_2O_2 into a more potent intoxicant (23). Moreover, our studies and those of others (19, 38) demonstrated that, when *S. aureus* has been completely killed, *S. pneumoniae* produced significantly less H_2O_2 (e.g., TIGR4, <200 μM) than the demonstrated minimal bactericidal concentration (MBC) of pure H_2O_2 (10 mM) for *S. aureus* strains (19, 38).

In this study, we used *in vitro* models mimicking *S. pneumoniae*-*S. aureus* cocolonization of the upper airways and demonstrated that an outcompeting density of *S. pneumoniae* was necessary to kill *S. aureus*. We also demonstrated that the interaction between *S. pneumoniae* and *S. aureus* stimulates the conversion of hydrogen peroxide into the strongest oxidative radical, hydroxyl (·OH), which reacts at nearly diffusion rates with most substrates, inducing DNA degradation and leading to the intoxication and death of *S. aureus* bacteria. The target(s) of the ·OH radicals represents an exciting new alternative for the development of therapeutics against *S. aureus* infections.

RESULTS

Contact-mediated killing of *S. aureus* by *S. pneumoniae* requires a threshold pneumococcal density. We previously demonstrated that killing of *S. aureus* strains by *S. pneumoniae* in liquid cultures required physical contact (23). We therefore reasoned that killing was likely to occur on solid media and designed a contact-mediated killing assay on blood agar plates. In this assay, we inoculated increasing densities of early-log-phase cultures of *S. pneumoniae* with different densities of *S. aureus* (i.e., 10^6 CFU/ml of *S. aureus* versus 10^6, 10^7, 10^8, or 10^9 CFU/ml of *S. pneumoniae*), and the plates were incubated overnight. In most mixtures where the density of *S. pneumoniae* outcompeted that of *S. aureus* by at least 2 log units (i.e., *S. pneumoniae*, 10^8 CFU/ml, and *S. aureus*, 10^6 CFU/ml), *S. pneumoniae* completely eradicated *S. aureus* (Fig. 1A). *S. pneumoniae* inoculated at 10^9 CFU/ml eradicated all *S. aureus* inocula. Similar results were obtained when two other *S. aureus* strains, NRS170 and NRS408, were assessed (not shown). To confirm the killing of *S. aureus* and the observed loss of chromosomal DNA observed by confocal microscopy (explained below), we isolated DNA from each mixture presented in Fig. 1A or single cultures (control). The DNA was used as a template in quantitative PCRs (qPCRs) targeting either *S. pneumoniae* or *S. aureus*. As expected, the number of genome equivalents (GenEqu) of *S. aureus* per milliliter did not change when the density outcompeted that of *S. pneumoniae* (not shown). When DNA was isolated from experiments where the *S. pneumoniae* density was greater than that of *S. aureus*, a density-dependent decrease of *S. aureus* GenEqu per milliliter was observed to a point where DNA from *S. aureus* was no longer detected (Fig. 1B to D; see Fig. S1 in the supplemental material). The number of GenEqu per milliliter of *S. pneumoniae* DNA (median, 1.4×10^9 GenEqu/ml) was not affected by incubation with

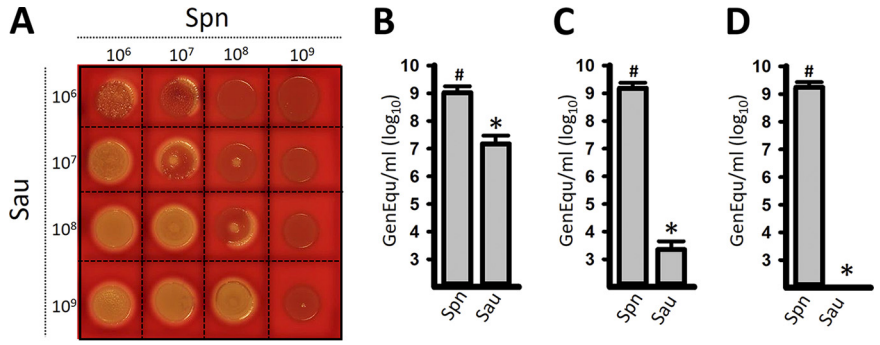

FIG 1 Contact-, and density-dependent killing of *S. aureus* (Sau) by *S. pneumoniae* (Spn). (A) *S. pneumoniae* strain TIGR4 and *S. aureus* strain Newman were inoculated concurrently at the indicated densities (CFU per milliliter). Once inoculated, the plates were incubated for 24 h at 37°C. (B to D) To quantify genome equivalents per milliliter of *S. pneumoniae* or *S. aureus*, bacteria growing on spots inoculated with 10^8 CFU/ml of *S. pneumoniae* and 10^8 (B), 10^7 (C), or 10^6 (D) CFU/ml of *S. aureus* were collected; DNA was extracted; and the DNA was used as a template in species-specific qPCRs. The error bars represent the standard errors of the means calculated using data from at least three independent experiments. *, $P < 0.05$ compared to *S. aureus* control incubated alone; #, $P > 0.67$ compared to *S. pneumoniae* control inoculated alone.

any density of *S. aureus*. Density-dependent killing of *S. aureus* was also confirmed by culture (see Fig. S2 in the supplemental material).

Confocal micrographs using antibodies against their capsules showed that, when inoculated at similar densities (i.e., ~10^6 CFU/ml), *S. pneumoniae* and *S. aureus* were observed intact and with areas of strong colocalization (Fig. 2, bottom row, arrowheads). DAPI (4′,6-diamidino-2-phenylindole) staining showed DNA from both species. In micrographs where *S. pneumoniae* outcompeted *S. aureus* (e.g., *S. pneumoniae*, ~10^7

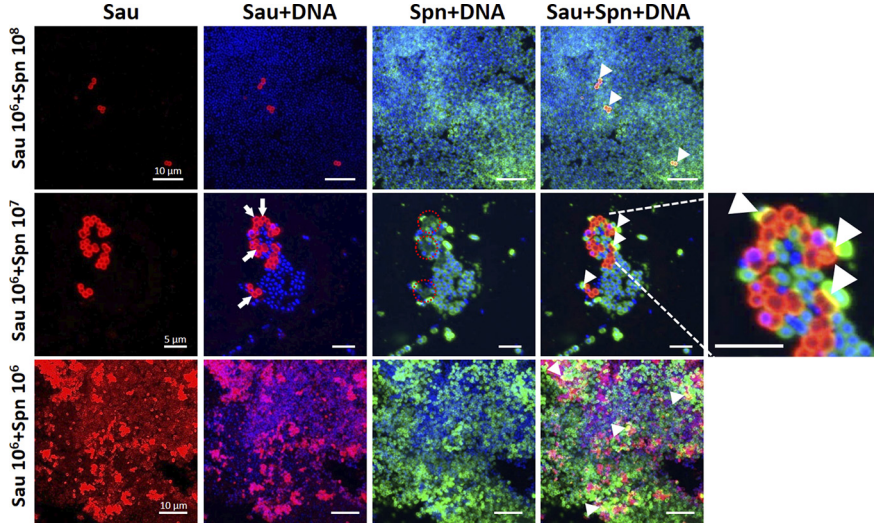

FIG 2 *S. pneumoniae* (Spn) contact-dependent killing of *S. aureus* (Sau) induces loss of DNA signal. Bacteria growing on blood agar plates from the experiments presented in Fig. 1, inoculated with the specific density of each species shown on the left, were imprinted onto glass slides. The preparations were fixed with paraformaldehyde, and *S. aureus* bacteria were stained with an anti-*S. aureus* antibody followed by an anti-rabbit Alexa Fluor 555-labeled antibody. *S. pneumoniae* was stained with an Alexa Fluor 488-labeled anti-*S. pneumoniae* antibody, while the DNA was stained with DAPI. The preparations were analyzed with a confocal microscope. Shown are 3D reconstructions of z stacks obtained from *xy* optical sections. The specific channel of each panel is shown at the top. The arrows point to *S. aureus* bacteria stained red with a loss of DNA signal, while the red dashed circles indicate areas where DNA signal is missing, corresponding to the arrows. The arrowheads show physical colocalization (yellow) of *S. aureus* and *S. pneumoniae*. The dimensions of the scale bars shown in the left column apply to all the images in the same row. The image on the far right was digitally enlarged to show details of the area indicated by the dashed lines.

CFU/ml versus *S. aureus*, ~10^6 CFU/ml), only a few *S. aureus* cells were observed in comparison to the abundant pneumococci (Fig. 2, middle and top rows). Moreover, three-dimensional (3D) reconstruction of z stacks revealed that, in the majority of *S. aureus* cells in mixtures with outcompeting *S. pneumoniae*, the DAPI signal was absent, suggesting that the DNA had been degraded (Fig. 2, arrows). Absence of DNA in *S. aureus* particularly coincided with the bacteria colocalizing with *S. pneumoniae* (Fig. 2, enlarged image). Together, these results identified dose- and contact-dependent killing of *S. aureus* by *S. pneumoniae* that included DNA degradation.

Differential sensitivities of *S. aureus* strains to killing by *S. pneumoniae*. Different *S. aureus* strains have distinct sensitivities to H_2O_2 killing; thus, it was possible that the results described above were not representative. We therefore tested a collection of 20 MRSA (including vancomycin-intermediate *S. aureus* [VISA]) and methicillin-susceptible *S. aureus* (MSSA) strains from seven clonal complexes (see Table S1 in the supplemental material) for their sensitivities to killing when incubated along with *S. pneumoniae*. To quantify the maximum density of *S. aureus* killed by *S. pneumoniae*, we utilized a microplate model with 4 h of coculture incubation at 37°C. All the *S. aureus* strains were killed by *S. pneumoniae*, but we noted statistically significant differences across strains ($P = 0.002$) (Fig. 3A). The most sensitive strain, NRS170, had a 426-fold difference ($P = 0.008$) in sensitivity to *S. pneumoniae* compared to the most resistant strain, NRS049 (Fig. 3A; see Table S1). Increased sensitivity of NRS170 to *S. pneumoniae* killing was also observed using the plate-killing model (not shown). The rest of the strains, including *S. aureus* strain Newman, showed linear distributions in their sensitivities to *S. pneumoniae* ($R^2 = 0.95$) that spanned an ~30-fold range. The variability among this group (excluding NRS170 and NRS408) was also statistically significant ($P = 0.05$). Surprisingly, there was no association between the clonal complex and sensitivity to *S. pneumoniae* (Fig. 3B).

Hydrogen peroxide has been implicated as the main factor produced by *S. pneumoniae* to kill *S. aureus* strains (14, 20). We hypothesized that the level of sensitivity of an *S. aureus* strain to H_2O_2 correlated with sensitivity to *S. pneumoniae* killing. Differential sensitivity to H_2O_2 was observed in our experiments, with the growth of some strains (i.e., NRS3 and NRS21) completely inhibited by H_2O_2 whereas a subset of strains were not susceptible at all to challenge with even 5 mM H_2O_2 (not shown). However, contrary to our hypothesis, the level of *S. pneumoniae* killing did not correlate with retardation of growth by H_2O_2 (Fig. 3C). These results showed that there was a complex genetic relationship between the ability to grow in the presence of hydrogen peroxide and the degree of sensitivity to *S. pneumoniae* killing. The finding that the genetic background (clonal complex) was not strongly associated with the level of killing suggests that recently acquired mutations may play a major role in determining the level of susceptibility of each individual *S. aureus* strain.

Resistant *S. aureus* strains can protect sensitive strains from killing by *S. pneumoniae*. To study the effect of *S. pneumoniae* sensitivity on *S. aureus* strain selection, we utilized one of the most sensitive strains (NRS408) and one of the most resistant strains (NRS049). Strain NRS049 was resistant to tetracycline, and we isolated an NRS408-derived rifampin-resistant mutant (NRS408J) to track the growth of the strain. There was a significant difference between strains NRS049 and NRS408J ($P < 0.05$) in *S. pneumoniae* sensitivity (Fig. 4A). There was no significant difference in NRS049 *S. pneumoniae* sensitivity measurements or NRS408 relative to NRS408J measurements between results presented in Fig. 3A and 4A. We then competed the resistant NRS049 strain and the sensitive NRS408J strain (5×10^6 CFU/ml of each strain, the minimum concentration at which NRS049 was predicted to survive) in the presence of TIGR4 (1.5×10^7 CFU/ml). While this dose of *S. pneumoniae* killed NRS408J but not the NRS049 strain, coincubation of the two *S. aureus* strains led to survival of both under *S. pneumoniae* challenge (Fig. 4B). Given that killing of *S. aureus* is density dependent, to determine whether this competition outcome was affected by the *S. aureus* strain density, we performed several endpoint *S. aureus* growth assays over a

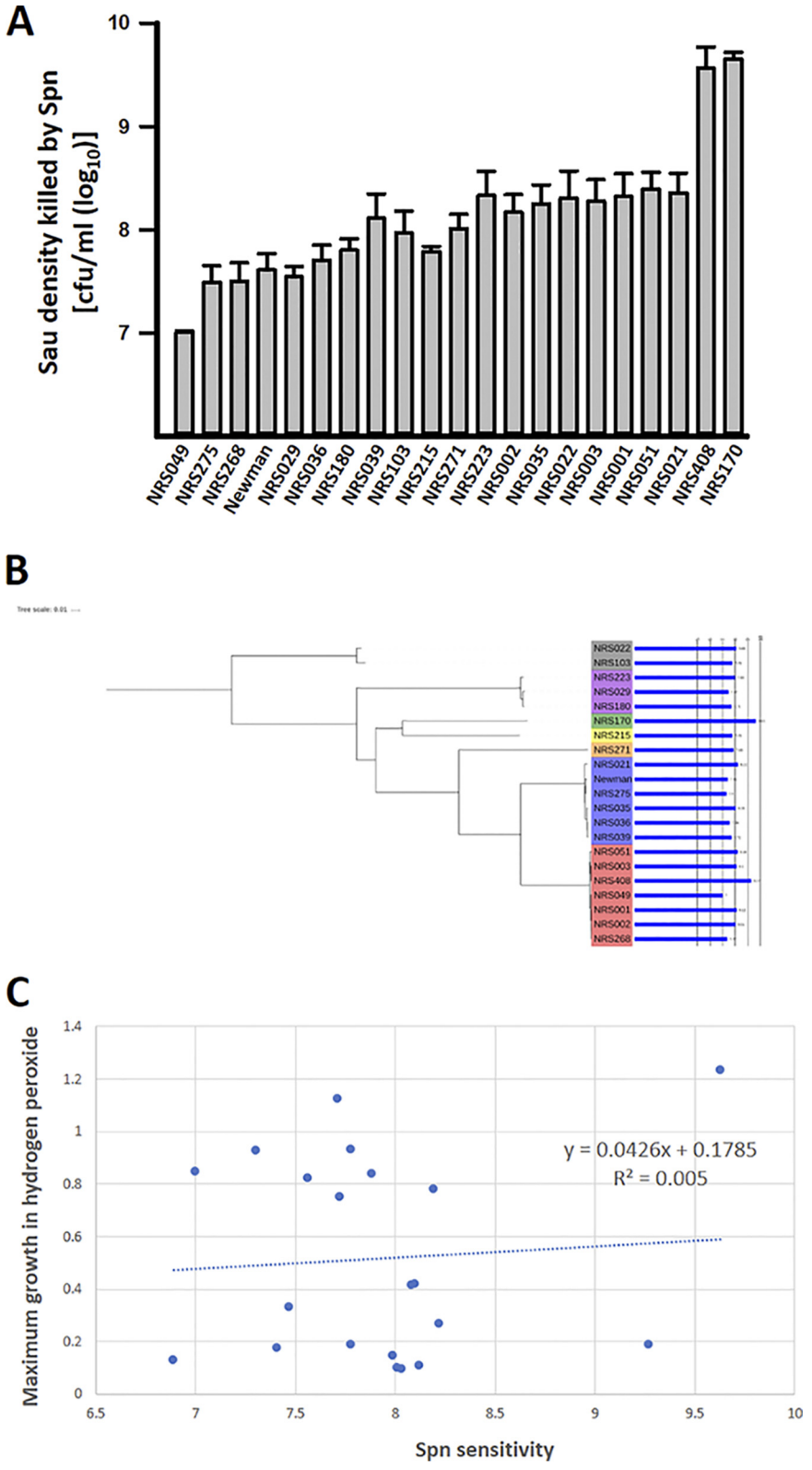

FIG 3 Variability in *S. aureus* (Sau) strain sensitivity to *S. pneumoniae* (Spn). (A) Decreasing densities of the indicated *S. aureus* strains spanning ~1×10^{10} and ~1×10^{6} CFU/ml were cocultured with 1.5×10^{7} CFU/ml of *S. pneumoniae* in THY and incubated for 4 h at 37°C. Cultures were serially diluted and plated on TSA supplemented with optochin. The maximum *S. aureus* inoculum completely killed by 1.5×10^{7} CFU/ml of *S. pneumoniae* was then determined from the maximum concentration killed. The standard errors of the mean of three independent experiments are shown. (B) Maximum-likelihood phylogeny of

(Continued on next page)

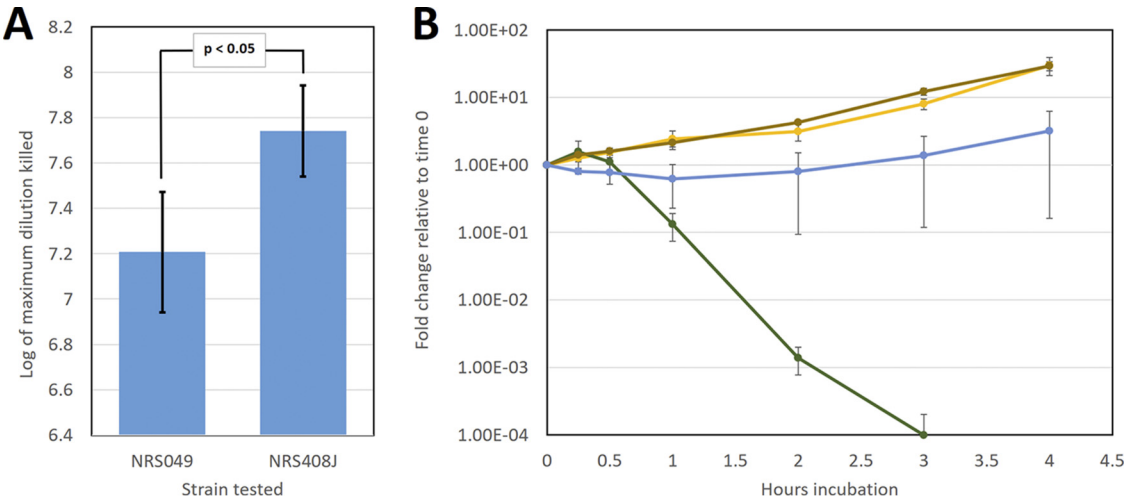

FIG 4 Competition between *S. pneumoniae*-sensitive and *S. pneumoniae*-resistant *S. aureus* strains in the presence of *S. pneumoniae*. (A) Sensitivities of *S. aureus* strains NRS049 and NRS408J to *S. pneumoniae* (TIGR4) killing. Sensitivity was measured as described in the legend to Fig. 3A. The results represent three biological replicates and two independent experiments. The results are presented with two standard errors above and below the mean. (B) Competition experiments between resistant (NRS049) and sensitive (NRS408J) *S. aureus* strains (5e6 CFU/ml) in the presence of *S. pneumoniae* (TIGR4; 1.5e7 CFU/ml). Strains NRS049, NRS408J, and TIGR4 at the previously stated doses were cocultured in THY for 4 h at 37°C without agitation. Coculture samples were collected at 0 min, 15 min, 30 min, 1 h, 2 h, 3 h, and 4 h. Coculture sample dilutions were then spotted on TSA supplemented with 16 μg/ml tetracycline or 4 μg/ml rifampin and grown overnight at 37°C to determine the concentrations of NRS049 and the NRS408 rifampin-resistant mutant (NRS408J) at corresponding time points. The fold change of the rifampin-resistant mutant NRS408J relative to time zero is shown with TIGR4 alone (green), TIGR4 and NRS049 (blue), NRS049 (brown), and the mutant itself alone (yellow). The results represent three biological replicates and are presented with one standard error above and one below the mean.

range of NRS049 and NRS408J densities (see Table S2 in the supplemental material). The sensitive NRS408J survived under all conditions under which the resistant NRS049 strain survived, regardless of whether the total *S. aureus* dose was 5×10^6 CFU/ml or more (see Table S2).

Mutations in *spxB* and *lctO* are required to inhibit *S. pneumoniae* killing of *S. aureus*. The experiments shown in Fig. 3 suggested that killing of *S. aureus* strains was not the sole consequence of exposure to H_2O_2. In *S. pneumoniae*, most H_2O_2 (~85%) is produced during the oxidation of pyruvate to acetyl-phosphate (acetyl~P) by SpxB (Fig. 5A). Although to a lesser extent, hydrogen peroxide is also produced during the oxidation of lactate to pyruvate by the enzyme LctO (Fig. 5A) (26). To gain insight into this contact-dependent, molecular-mechanism-mediated killing of *S. aureus*, we generated single Δ*spxB* and Δ*lctO* mutants and a Δ*spxB* Δ*lctO* double mutant in TIGR4. We then assessed killing of *S. aureus* by these mutants using our density-controlled experimental models. When incubated along with ~10^7 CFU/ml *S. aureus* in the contact-dependent plate model, the TIGR4 Δ*lctO* mutant killed *S. aureus* to the same extent as the TIGR4 wild-type strain at all tested *S. pneumoniae* densities (Fig. 5B). At a density of ~10^7 CFU/ml, TIGR4 Δ*spxB* did not kill *S. aureus*. Surprisingly, TIGR4 Δ*spxB* killed *S. aureus* when we increased the challenge density to >10^8 CFU/ml (Fig. 5B). *S. pneumoniae* strain Pn20, isolated from the nasopharynx of a child (20), and its Δ*spxB* mutant derivative were also tested with essentially similar results (i.e., an increased density killed *S. aureus* [data not shown]). Furthermore, a similar 100-fold-increased density of TIGR4 Δ*spxB* killing *S. aureus*, in comparison to the TIGR4 wild type, was observed when another *S. aureus* strain, NRS049, was challenged (Fig. 5C). These results

FIG 3 Legend (Continued)
strains tested with $\log_{10}$ bactericidal efficiency of *S. pneumoniae* plotted as a bar chart. The clonal complex designation of each strain is shown by the color range. (C) Maximum growth (OD_{600} measured after 12 h of incubation at 37°C) in hydrogen peroxide (2.5 mM)-supplemented TSB plotted against *S. pneumoniae* sensitivity of the corresponding strain. The values represent averages from at least three replicates for each strain.

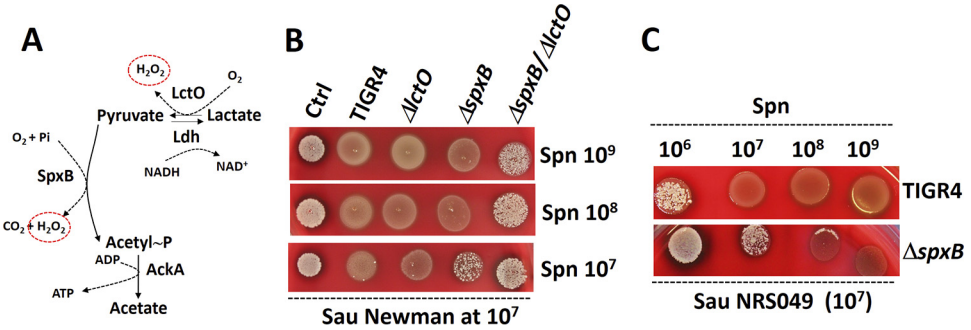

FIG 5 *S. pneumoniae* (Spn) contact-mediated killing of *S. aureus* (Sau) requires enzymes SpxB and LctO. (A) Oxidation of pyruvate to acetyl~P by the enzyme pyruvate oxidase (SpxB). The reaction uses molecular O_2 and inorganic phosphate (P_i), producing CO_2 and H_2O_2 (circled). Acetyl~P is then converted to acetyl coenzyme A by acetate kinase (AckA) in a reaction that produces ATP. The enzyme lactate oxidase (LctO) catalyzes the formation of pyruvate from lactate, producing H_2O_2. (B) *S. pneumoniae* strains TIGR4, TIGR4 Δ*lctO*, TIGR4 Δ*spxB*, and TIGR4 Δ*spxB* Δ*lctO* were inoculated on blood agar plates at the densities indicated on the right (CFU per milliliter) concurrently with *S. aureus* strain Newman, which was inoculated at a density of ~10^7 CFU/ml. (C) *S. pneumoniae* strains were inoculated at the densities shown at the top concurrently with *S. aureus* strain NRS049, inoculated at ~10^7 CFU/ml. The agar plates were incubated overnight at 37°C.

suggested that H_2O_2 generated by LctO was sufficient to induce killing of *S. aureus*. Confirming this, the TIGR4 Δ*spxB* Δ*lctO* mutant was unable to kill *S. aureus* even at a high density of ~10^9 CFU/ml (Fig. 5B).

We then used the microplate model to quantitatively assess *S. aureus* killing by these mutant strains. Experiments revealed that neither planktonic *S. aureus* nor biofilm *S. aureus* cells were killed by TIGR4 Δ*spxB* in comparison with the wild-type strain (Fig. 6A and B). The same phenotype was observed when two other independent TIGR4-derived Δ*spxB* mutants were tested (see Fig. S3 in the supplemental material). Similar to what we observed using the plate model, the TIGR4 Δ*lctO* mutant killed *S. aureus* strains at rates similar to that of wild-type TIGR4 (Fig. 6A and B). As expected, as a mutation in *spxB* was enough to block *S. aureus* killing in this model, the Δ*spxB* Δ*lctO* double mutant was unable to kill *S. aureus* strain Newman (not shown). Under the culture conditions utilized (i.e., incubation in Todd-Hewitt broth containing 0.5% [wt/vol] yeast extract [THY], with environmental oxygen and 5% CO_2), *S. pneumoniae* strains TIGR4 and TIGR4 Δ*lctO* produced, after 4 h of incubation, ~180 μM and ~140 μM H_2O_2, respectively (Table 1). Cultures of three different *spxB* mutants, however, yielded undetectable levels of hydrogen peroxide (Table 1). Overall, our experiments demonstrated that both H_2O_2-producing enzymes, SpxB and LctO, contribute to the contact-dependent killing of *S. aureus* strains.

A hydroxyl radical (·OH) is generated during the interaction between *S. pneumoniae* and *S. aureus* to rapidly kill *S. aureus*. Given that our experiments demonstrated that even ~5 mM pure H_2O_2 did not affect the viability of some *S. aureus* strains (Fig. 3) but that cultures of the same strains were killed by *S. pneumoniae* producing ~36-fold less H_2O_2 (i.e., ~140 μM), the possibility was raised that SpxB/LctO-produced H_2O_2 was converted into the ·OH radical. To test this hypothesis, we first conducted a dose-response study to identify three sublethal doses of H_2O_2 for *S. aureus*, 1.0, 1.2, and 1.4 mM (Fig. 7). For example, 1 mM H_2O_2 allowed the survival of $>1 \times 10^6$ CFU/ml *S. aureus* when challenged against three different *S. aureus* strains (Fig. 7). We reasoned that if H_2O_2 is converted to a hydroxyl radical, then incubating *S. aureus*, TIGR4 Δ*spxB* (which does not produce significant amounts of H_2O_2), and a sublethal dose of H_2O_2 would allow killing. As shown in Fig. 7, the density of any of the three *S. aureus* strains incubated with TIGR4 Δ*spx*B was similar to the density in control wells containing *S. aureus* alone (Fig. 7A to C). Incubation of *S. aureus*; TIGR4 Δ*spxB*; and 1.0, 1.2, or 1.4 mM H_2O_2 was sufficient to completely eradicate cultures of *S. aureus* strain Newman, NRS408, and NRS049, respectively. Experiments with *S. aureus* strain Newman incubated with TIGR4 Δ*spxB* Δ*lctO* and 1 mM H_2O_2 showed essentially the same result

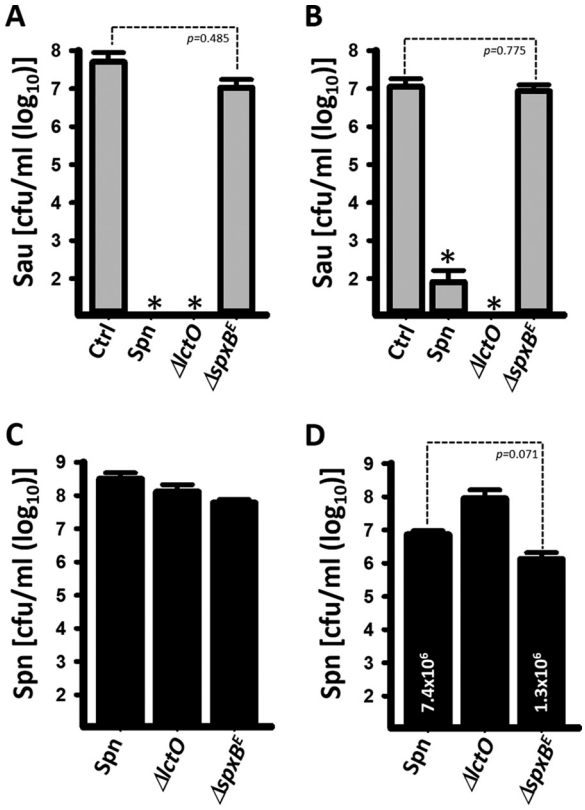

FIG 6 A mutation in *spxB*, but not in *lctO*, renders *S. pneumoniae* (Spn) unable to kill *S. aureus* (Sau) in a microplate model. *S. aureus* strain Newman ($\sim 1 \times 10^6$ CFU/ml) was inoculated alone (Ctrl) or along with the indicated *S. pneumoniae* strains ($\sim 1 \times 10^6$ CFU/ml) in microplates containing THY and incubated for 4 h at 37°C. Bacteria were harvested and then diluted and plated onto SMA (A and B) or BAP with gentamicin (C and D) to obtain counts of *S. aureus* planktonic cells (A), *S. aureus* biofilms (B), *S. pneumoniae* planktonic cells (C), or *S. pneumoniae* biofilms (D). The error bars represent the standard errors of the means calculated using data from at least three independent experiments. (A and B) *, $P < 0.05$ compared to *S. aureus* control incubated alone. (D) For comparison, the median (CFU per milliliter) is shown inside two of the bars.

(Fig. 7D). These experiments strengthened our hypothesis that H_2O_2 was converted into a hydroxyl radical (·OH).

Thiourea (15 mM), sodium salicylate, and dimethyl sulfoxide (Me_2SO [300 mM]), are specific ·OH scavengers (34); thiourea and Me_2SO reduced H_2O_2 killing of *S. aureus* by 98% and 38%, respectively (34). As shown in Fig. 8A, incubating *S. aureus* strain Newman, *S. pneumoniae*, and 10 mM thiourea was enough to significantly inhibit killing of *S. aureus*, whereas 20 mM and 40 mM completely inhibited H_2O_2-mediated killing. The density of *S. pneumoniae* was not affected by incubation with any amount of thiourea (Fig. 8B). Similar protection from challenge with *S. pneumoniae* was conferred on *S. aureus* by incubating the two species, along with a scavenger of hydroxyl radicals, Me_2SO (Fig. 8C and D) or sodium salicylate (see Fig. S4 in the supplemental material).

TABLE 1 Production of H_2O_2 by TIGR4 and isogenic derivative mutants

Strain	Production of H_2O_2 at (h):			
	0	1	2	4
TIGR4	5.7 μM	35.6 μM	50.3 μM	179.6 μM
TIGR4 Δ*lctO*	<50 nM[a]	9.9 μM	45.1 μM	136.3 μM
TIGR4 Δ*spxB*^{U}	<50 nM	<50 nM	<50 nM	<50 nM
TIGR4 Δ*spxB*^{E}	<50 nM	<50 nM	<50 nM	<50 nM
TIGR4 Δ*spxB*^{E} Δ*lctO*	<50 nM	<50 nM	<50 nM	<50 nM

[a]Limit of detection.

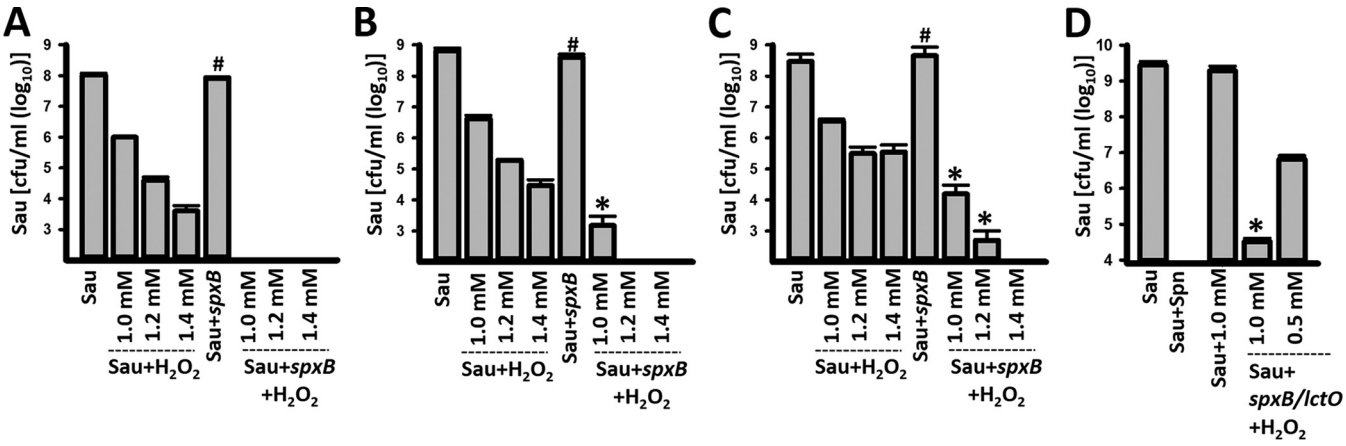

FIG 7 *S. pneumoniae* (Spn) produces a stronger oxidant from H_2O_2 to kill *S. aureus* (Sau) strains. *S. aureus* strain Newman (A and D), NRS408 (B), or NRS049 (C) was incubated alone at a density of $\sim 1 \times 10^6$ CFU/ml, with the indicated molarity of H_2O_2, TIGR4 Δ*spxB* ($\sim 1 \times 10^6$ CFU/ml), TIGR4 Δ*spxB* ($\sim 1 \times 10^6$ CFU/ml) and H_2O_2 or with TIGR4 Δ*spxB lctO* ($\sim 1 \times 10^6$ CFU/ml). Bacteria were incubated for 4 h at 37°C and then harvested, diluted, and plated on SMA to obtain counts of *S. aureus*. The error bars represent the standard errors of the means calculated using data from at least three independent experiments. *, $P < 0.05$ compared to the corresponding concentration of H_2O_2; #, $P > 0.30$ compared to *S. aureus* control incubated alone.

To identify the *in vivo* formation of hydroxyl radicals, we utilized the α-(4-pyridyl-1-oxide)-*N-tert*-butyl nitrone (4-POBN)–ethanol spin-trapping system. Figure 9 shows a marked increase in the hydroxyethyl radical spin adduct in bacterial cells of the TIGR4 wt in comparison to signals from a reaction mixture containing TIGR4 wt cells and a

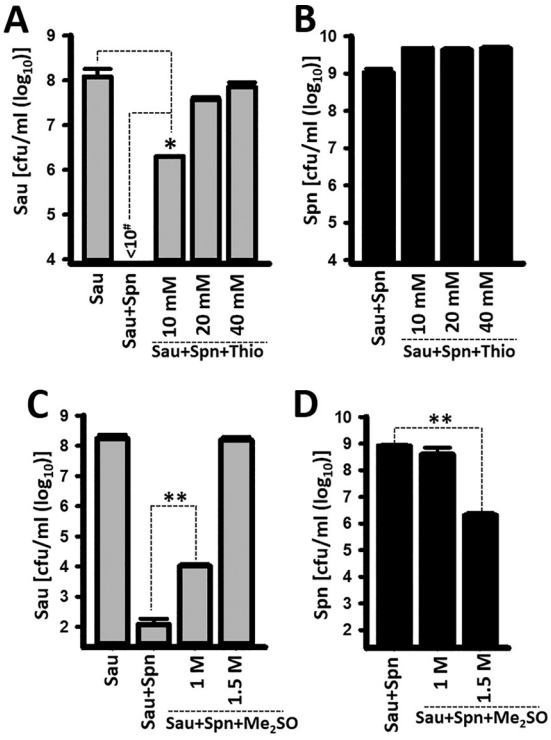

FIG 8 Scavengers of ·OH block *S. pneumoniae* (Spn)-induced killing of *S. aureus* (Sau). *S. aureus* strain Newman was inoculated ($\sim 1 \times 10^6$ CFU/ml) alone, with *S. pneumoniae* TIGR4 ($\sim 1 \times 10^6$ CFU/ml), with *S. pneumoniae* and thiourea (Thio), or with *S. pneumoniae* and Me_2SO. After 4 h of incubation at 37°C, bacteria were harvested, diluted, and plated to obtain counts of *S. aureus* (A and C) or *S. pneumoniae* (B and D). The error bars represent the standard errors of the mean calculated using data from at least three independent experiments. *, $P < 0.05$ compared with *S. aureus* control; **, $P < 0.0005$ compared to the density of *S. aureus* incubated with *S. pneumoniae*; #, limit of detection.

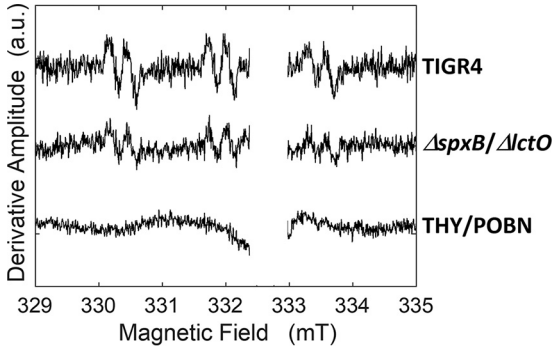

FIG 9 Detection of ·OH radicals in pneumococci by 4-POBN and DETAPAC-ethanol spin trapping. Shown are the EPR spectra of 4-POBN spin trapping in wild-type and double-mutant samples and, for comparison, a medium-only sample. The unassigned signal near the free-electron g value of 2.0023 (333.0 mT) was deleted. The EPR conditions were as follows: microwave frequency, 9.346 GHz; microwave power, 10 mW; modulation amplitude, 0.2 mT; modulation frequency, 100 kHz; temperature, 295 K. The spectra of wild-type and double-mutant samples represent an average of 96 scans minus the bacterial-medium spectrum. The bacterial-medium spectrum represents an average of 224 scans, with polynomial baseline correction. The spectra were baseline corrected using a polynomial function.

reaction mixture with bacterial cells harvested from cultures of the TIGR4 Δ*spxB* Δ*lctO* double mutant.

DISCUSSION

We have demonstrated in this study that the interaction between *S. pneumoniae* and *S. aureus* stimulates the conversion of H_2O_2 into a stronger oxidant, the hydroxyl radical, ·OH, to rapidly kill *S. aureus* bacteria. The toxic effects of several pneumococcal strains against *S. aureus* have been documented (14, 19, 20, 23, 27, 38). Hydrogen peroxide had long been believed to be the killing factor, but contrasting data suggesting that H_2O_2 was not required for killing have been published in the last few years (23, 30–32). Compelling evidence within this study has now identified highly reactive ·OH radicals generated from H_2O_2, because of interaction between the species, as the effector of such a mechanism. Given that H_2O_2 is permeable but a sublethal dose of H_2O_2 killed *S. aureus* strains when incubated along with H_2O_2-deficient *S. pneumoniae* strains, the conversion to ·OH radicals may be facilitated by pneumococcal cells. Certainly, other possibilities exist, including increased free Fe^{2+} in *S. aureus* due to the interaction with *S. pneumoniae*, which could be the result of stimulated iron uptake. The ·OH generated reacts at nearly diffusion-limited rates near the site of its generation (22, 39).

Although *S. aureus* can also produce H_2O_2, its potent catalase fully scavenges the H_2O_2 before it can cross the cytoplasmic membrane, and therefore, levels of hydrogen peroxide in the supernatant are undetectable (19). Intracellular levels of H_2O_2 in *S. aureus* have not been investigated, but in *E. coli*, these levels are maintained at 0.1 to 0.2 μM during aerobic growth (40). Therefore, the experiments in this study, along with data from other laboratories (14, 19, 20, 31, 41), support a model where *S. pneumoniae* secretes large amounts of H_2O_2 near *S. aureus* bacteria—but beyond a concentration that catalase would successfully scavenge—and then, due to a still unknown mechanism, it is rapidly converted into ·OH radicals that intoxicate *S. aureus* cells. We hypothesize that the target(s) of ·OH radicals on *S. aureus* cells is absent in pneumococci, and therefore, *S. pneumoniae* is less susceptible to these radicals (see below for more details). *S. aureus* intoxication with ·OH radicals may be accompanied by degradation of DNA, as confocal micrographs and quantitative PCRs demonstrated absence of DNA in *S. aureus* bacteria incubated with H_2O_2-producing *S. pneumoniae*. Hydroxyl radicals attack at the sugar or the base of the DNA, leading to sugar fragmentation, base loss, and a strand break with a terminal fragmented sugar residue (42). The resistance of *S. pneumoniae* to DNA damage has been speculated to occur by sequestration of Fe^{2+}, required to produce ·OH through the Fenton reaction, away from its DNA (22).

Animal studies demonstrated that *S. pneumoniae* (TIGR4) and *S. aureus* (Newman) cohabited in the nasal cavities of rats when the strains were inoculated at the same density (30, 31). One would expect that in this animal cocolonization model, only *S. pneumoniae* would be able to colonize, but this outcome did not occur. Instead, coinoculation of wild-type *S. pneumoniae* did not affect colonization by *S. aureus*, and neither a mutation in the pneumococcal *spxB* gene nor a mutation in the *S. aureus katG* gene (encoding catalase) had a positive or negative effect, respectively, on *S. aureus* density. If *S. pneumoniae* kills *S. aureus*, why did they cocolonize? Experiments in this study offer an explanation. When TIGR4 and *S. aureus* strain Newman were inoculated at similar densities, *S. aureus* in fact survived the challenge with *S. pneumoniae* (Fig. 1). However, with an outcompeting density of *S. pneumoniae*, staphylococci succumbed to the challenge. The killing was negated when *S. aureus* was incubated with the hydrogen peroxide production-defective *S. pneumoniae* Δ*spxB* Δ*lctO* mutant. We speculate that, in the surface-bound environment of the nasal cavity of rats or in the plate model, the close proximity of *S. pneumoniae* to *S. aureus* allows inactivation of H_2O_2 by the *S. aureus*-produced catalase but that increased production of H_2O_2 (i.e., by outcompeting pneumococci) overcomes the catalase-mediated inactivation, and thus, H_2O_2 is converted into $^{\cdot}OH$ radicals. We hypothesize that the conflicting results obtained in population studies where a negative association, or no association, has been demonstrated between concurrent carriage (i.e., colonization) of *S. pneumoniae* and *S. aureus* would have been resolved if the density of the strains had been taken into consideration.

The finding that the level of sensitivity is variable across *S. aureus* strains (Fig. 3A) and the surprising result that *S. pneumoniae* and H_2O_2 sensitivity in *S. aureus* are not correlated (Fig. 3B) suggest that other, undiscovered factors modulate *S. aureus* killing. We found that *S. aureus* strains can apparently cross-protect in mixtures, suggesting that a diffusible molecule is possibly involved. This result needs to be followed up in future work. Since the phenotype is variable across *S. aureus* strains without being closely linked to a particular clade, it may be possible to identify the genetic loci responsible by using a hypothesis-free genome-wide association study (GWAS) approach.

Studies conducted with *E. coli* demonstrated that H_2O_2-mediated killing occurred only in actively metabolizing cells (35, 42). Exogenously added H_2O_2 also kills *S. aureus* strains with a calculated 90% lethal dose (LD_{90}) and MBC of ~10 mM (19, 34). A 10-fold decrease in the sublethal concentration was determined and utilized in our studies (presented in Fig. 7) against strain Newman and two MRSA strains. The membrane-permeable H_2O_2 enters bacterial cells, reacting with the intracellular Fe^{2+} by Fenton reactions to produce $^{\cdot}OH$ radicals (34). The concentration of H_2O_2 quantified in the supernatant of *S. pneumoniae* to reach the LD_{90}, however, was ~7-fold lower (~140 μM) than a sublethal dose of exogenous H_2O_2 and ~70-fold lower than the LD_{90} of exogenously added H_2O_2 (~10 mM). This decreased amount of H_2O_2 in the *S. pneumoniae* supernatant, the fact that an H_2O_2 production-defective strain, when incubated with a sublethal dose of H_2O_2 (~1 mM), killed *S. aureus* strains, our experiments showing that *S. aureus* killing was blocked by hydroxyl scavengers, and spin-trapping experiments supported the hypothesis that production of $^{\cdot}OH$ radicals was stimulated by the interaction between pneumococcal cells and *S. aureus*.

Given that H_2O_2 targets metabolically active (i.e., respiring) *E. coli* cells (35) and that *S. aureus* undergoes cellular respiration whereas *S. pneumoniae* does not encode proteins of the respiratory chain (43), we speculate that hydroxyl radicals either target a component(s) of the respiratory chain or require a reducing equivalent from the respiratory chain to generate toxic hydroxyl radicals. In fact, the pneumococcus could be intoxicated by incubating it with increasing amounts of H_2O_2, but it required at least 10 mM H_2O_2 to completely eradicate *S. pneumoniae* bacteria. A challenge with such a large amount of H_2O_2 was partially inhibited by incubation with the $^{\cdot}OH$ scavenger thiourea (see Fig. S4 in the supplemental material).

An investigation by Selva et al. suggested that H_2O_2-mediated interference was triggered by lysogenic *S. aureus* phages, although in their study they obtained a 3- to

TABLE 2 Pneumococcal and staphylococcal strains used in this study

Strain	Description[a]	Reference(s) or source
TIGR4	Invasive clinical isolate; phenotype CSP2; capsular serotype 4	43
TIGR4 Δ*spxB*^{H}	TIGR4 with an insertion within the *spxB* gene; *spxB*::*kan-rpsL*$^{+}$	20, 27
TIGR4 Δ*spxB*^{U}	TIGR4 with a deletion of the *spxB* gene by transformation of *erm*(B); Ery^{r} cassette	13
SPJV29 (TIGR4 Δ*spxB*^{E})	TIGR4 with a deletion of the *spxB* gene by transformation of *erm*(B); Ery^{r} cassette	This study
TIGR4 Δ*lctO*	TIGR4 with a deletion of the *lctO* gene by transformation of a spectinomycin cassette	This study
TIGR4 Δ*spxB* Δ*lctO*	TIGR4 Δ*spxB*^{U} with a deletion of the *lctO* gene by transformation of a spectinomycin cassette	This study
Pn20	Serotype 35*B*; nasopharyngeal human isolate	20
Pn20Δ*spxB*	Pn20 Δ*spxB*::*kan-rpsL*$^{+}$ by transformation with PCR product of TIGR4 Δ*spxB*^{H}	20
S. aureus Newman	NCTC 8178, ATCC 13420	56
NRS408J	*S. aureus* NRS408 spontaneous rifampin-resistant mutant	This study
RN4220	*S. aureus* Hla^{-} nonlysogenic strain	57

[a]Ery^{r}, erythromycin resistance; H, *spxB* mutant strain obtained from M. Lipsitch at Harvard; U, *spxB* mutant strain prepared by C. J. Orihuela's group at UAB; E, *spxB* mutant prepared at Emory University (SPJV29).

4-log-unit reduction in *S. aureus* density, but not eradication, under similar culture conditions (41). Whereas some *S. aureus* strains utilized in the current study may be lysogenic, we tested a nonlysogenic *S. aureus* strain (RN4220) and obtained density-dependent, SpxB/LctO-dependent killing (data not shown). The detailed mechanism(s) and its target(s) are under active investigation in our laboratories. The target(s) of the ·OH radicals represents an exciting new alternative for the development of therapeutics against *S. aureus* infections.

MATERIALS AND METHODS

Bacterial strains and culture media. The *S. pneumoniae* and *S. aureus* wild-type strains and mutant derivatives utilized in this study are listed in Table 2. *S. pneumoniae* strains were cultured on blood agar plates (BAP) or BAP with 25 μg/ml gentamicin, whereas *S. aureus* strains were grown on salt mannitol agar (SMA) plates or tryptic soy agar (TSA) plates with or without 5 μg/ml optochin or on Luria-Bertani agar (LBA) (1% tryptone [Becton-Dickinson], 0.5% yeast extract, 1% NaCl, and 1.5% agar [Becton-Dickinson]). THY was utilized in all the experiments.

Preparation of inoculum for experiments. The inoculum was prepared essentially as previously described (44, 45). Briefly, an overnight BAP (for *S. pneumoniae*) or LBA (for *S. aureus*) culture was used to prepare a cell suspension in THY broth to an optical density at 600 nm (OD_{600}) of ~0.08. This suspension was incubated at 37°C in a 5% CO_2 atmosphere until the culture reached an OD_{600} of ~0.2 (early log phase). Then, glycerol was added to give a final 10% (vol/vol) concentration, and the suspension was stored at −80°C until it was used. An aliquot of these stocks was further diluted and plated to obtain bacterial counts (CFU per milliliter).

Mixed-culture killing assay on plates. Blood agar plates were coinoculated with both *S. pneumoniae* and *S. aureus* strains at different densities ranging from ~10^6 through ~10^9 CFU/ml. The inoculated plates were then incubated at 37°C in a 5% CO_2 atmosphere overnight. A creamy-yellow color on the BAP culture and the presence of a beta-hemolytic halo around each culture indicated growth of *S. aureus*. To quantify the densities of strains, cultures were harvested and an aliquot was diluted and plated to obtain bacterial counts, whereas DNA was extracted from another aliquot using a QIAamp DNA minikit (Qiagen) according to the manufacturer's instructions. DNA preparations were eluted with 100 μl of elution buffer, quantified using a Nanodrop spectrophotometer, and stored at −80°C until they were used.

Quantitative PCRs. Strain-specific qPCRs were performed to measure the densities of strains. Primers, probes, and the concentrations utilized are listed in Table 3. The total *S. pneumoniae* density was quantified using the panpneumococcus *lytA* assay (46), and detection of the *nuc* gene was used to quantify *S. aureus* density (47). Reactions were run along with serially diluted DNA standards corresponding to 4.29×10^5, 4.29×10^4, 4.29×10^3, 4.29×10^2, 4.29×10^1, and 2.14×10^1 genome equivalents of *S. pneumoniae* or 3.29×10^5, 3.29×10^4, 3.29×10^3, 3.29×10^2, 3.29×10^1, and 3.14×10^1 genome equivalents of *S. aureus*. Reactions were carried out using a Bio-Rad CFX96 Touch real-time PCR detection system (Bio-Rad, Hercules, CA) and the following cycling parameters: 50°C for 2 min, 95°C for 2 min, and 40 cycles of 95°C for 15 s and 60°C for 1 min. The final numbers of genome equivalents per milliliter were calculated using the CFX software (Bio-Rad, Hercules, CA).

Determination of *S. aureus* strain sensitivity to *S. pneumoniae*. Inocula of *S. aureus* strains prepared as stated above, with known densities, were serially diluted in THY to generate inocula. Decreasing densities of *S. aureus* strains were inoculated along with 1.5×10^7 CFU/ml of *S. pneumoniae* and incubated for 4 h in 96-well microplates. The cultures were diluted and plated on TSA supplemented with optochin (5 μg/ml). The highest density of each *S. aureus* strain killed by 1.5×10^7 CFU/ml of *S. pneumoniae* within 4 h was then determined.

Competition between resistant and sensitive *S. aureus* strains under *S. pneumoniae* selection. For the competition experiments, we prepared an NRS408-derived rifampin-resistant mutant (NRS408J) by plating an overnight tryptic soy broth (TSB) culture concentrated 10-fold on a TSA plate supplemented with 4 μg/ml rifampin. *S. pneumoniae* strain TIGR4 (1.5×10^7 CFU/ml) was then cocultured in

TABLE 3 Primers and probes used in this study

Target	Primer or probe sequence (5′–3′)[a]	Reference
S. pneumoniae lytA	F, ACGCAATCTAGCAGATGAAGCA R, TCGTGCGTTTTAATTCCAGCT Probe, FAM-TGCCGAAAACGCTTGATACAGGGAG	46
S. aureus nuc	F, GTTGCTTAGTGTTAACTTTAGTTGTA R, AATGTCGCAGGTTCTTTATGTAATTT Probe, HEX-AAGTCTAAGTAGCTCAGCAAATGCA	47
UP_spxB_DN	F, TATCAATCACGCTCCTGC R, CTCGTTATGGACAATGCT	13
XbaI-erm(B)-XhoI	F, CAGTCTAGAAAAAATTTGTAATTAAGAAGGAGT R, CAGCTCGAGCCAAATTTACAAAAGCGACTCA	This study
lctO_UP-FW	TGGAAAGTAGGCATCAGC	This study
lctO_UP (SpI_KnSpc)-RV	**TCCTCCTCACTATTTTG**ATAAACTGTCCTCCTCG	This study
lctO_DN (SpI_KnSpc)-FW	**TGGAAACACTTCGTGAA**GACTTAAAATTGTATTG	This study
lctO_DN-RV	CGTAATTCCACTTGATCC	This study
SpcK7-FW	CAAAATAGTGAGGAGGA	This study
SpcK7-RV	TTCACGAAGTGTTTCCA	This study

[a]F, forward; R, reverse; FAM, 6-carboxyfluorescein; HEX, 6-carboxy-2,4,4,5,7,7-hexachlorofluorescein. Sequences overlapping the spectinomycin resistance cassette are in boldface.

THY with three different mixtures of *S. aureus* strains (5×10^6 CFU/ml of each *S. aureus* strain). A mixture contained NRS049, NRS408J, or both strains NRS049 and NRS408J. Experiments with negative controls without *S. pneumoniae* were performed for each of the *S. aureus* strain mixtures. All the cultures (3 ml each) were incubated without shaking at 37°C in a 5% CO_2 atmosphere. Cocultures were sampled at 0-, 15-, and 30-min and 1-, 2-, 3-, and 4-h time points. Sample dilutions were then spotted on TSA plates supplemented with 16 μg/ml tetracycline or 4 μg/ml rifampin to detect NRS049 and the NRS408 rifampin-resistant mutant (NRS408J), respectively. The following day, spot colonies were enumerated to calculate the number of residual CFU per milliliter at each time point.

Growth curves and hydrogen peroxide sensitivity. Strains were grown at 37°C in TSB or TSB supplemented with 0.1, 2.5, or 5.0 mM H_2O_2. The initial ODs were normalized to between 0.1 and 0.2 (roughly a 1/100 dilution of the overnight culture) readings from a microplate reader (Eon; BioTek, Inc.) before the growth curves were performed. Growth curves (OD_{600}) were determined in a plate reader collecting data every 10 minutes for up to 12 h.

Confocal-microscopy studies. Bacteria grown in experiments performed using the plate model (Fig. 1A) were imprinted onto rounded glass slides and immediately fixed with 2% paraformaldehyde (PFA) for 15 min at room temperature. The fixed bacteria were then blocked with 1% bovine serum albumin (BSA) for 30 min at 37°C and incubated first with a rabbit polyclonal anti-*S. aureus* antibody (4 μg/ml; Santa Cruz Biotechnology, Inc.) for 1 h at room temperature, followed by phosphate-buffered saline (PBS) washes and 1 h of incubation with a secondary Alexa Fluor 555-labeled goat anti-rabbit antibody (20 μg/ml; Molecular Probes). The preparation was then washed with sterile PBS and incubated for 30 min with anti-*S. pneumoniae* antibodies raised in rabbit (Statens Serum Institute) that had been previously labeled with Alexa Fluor 488 (50 μg/ml; Molecular Probes). The stained preparations were finally washed twice with PBS, mounted with ProLong Diamond antifade mountant with DAPI (Molecular Probes), and analyzed with an Olympus FV1000 confocal microscope. The confocal images were analyzed with Image J version 1.49k (National Institutes of Health).

Preparation of TIGR4-derived Δ*spxB*, Δ*lctO*, and Δ*spxB* Δ*lctO* mutants. Isogenic *spxB* mutant derivatives of *S. pneumoniae* strain TIGR4 (43) were prepared as described in our recent publication (13). A deletion within the *lctO* gene in the wild-type TIGR4, or TIGR4 Δ*spxB*, was generated using a cassette containing *lctO* upstream (lctO_UP-FW and lctO_UP-RV) and downstream (lctO_DN-FW and lctO_DN-RV) sequences and the spectinomycin resistance gene (SpcK7-FW and SpcK7-RV). This cassette was prepared by splicing overlap extension PCR with primers (in parentheses above and listed in Table 3) (48, 49) and transformed into pneumococci using standard procedures (50). BAP with spectinomycin (100 μg/ml) or erythromycin (0.5 μg/ml) was used to select *lctO* or *spxB* mutants, respectively. All deletions were confirmed by PCR and sequencing.

Microplate model to investigate killing of *S. aureus* by *S. pneumoniae* strains. An *S. pneumoniae* strain was inoculated along with *S. aureus* strain Newman at a density of $\sim 1 \times 10^6$ CFU/ml in a 6-well microplate containing THY and incubated for 4 h at 37°C in a 5% CO_2 atmosphere. Control wells were inoculated with only *S. pneumoniae* or only *S. aureus*. In another set of experiments, *S. aureus* was inoculated, along with increasing amounts of hydrogen peroxide (Sigma), with the TIGR4 Δ*spxB*^{E} (SPJV29) mutant alone or with TIGR4 Δ*spxB*^{E} and hydrogen peroxide. Technical duplicates were included throughout these experiments. At the end of the incubation, planktonic cells were removed, diluted, and plated onto BAP with gentamicin to obtain the number of CFU of *S. pneumoniae* per milliliter or onto LBA plates with optochin to obtain the number of CFU of *S. aureus* per milliliter. The biofilms were washed once with PBS, resuspended

in 1 ml of sterile PBS, and sonicated for 15 s using a Bransonic ultrasonic water bath (Branson, Danbury, CT), followed by extensive pipetting to remove the remaining attached biofilm bacteria. The biofilms were then diluted and plated as described above. Experiments were repeated three times.

Quantifying production of hydrogen peroxide. *S. pneumoniae* strains were inoculated at a density of ~1 × 10^6 CFU/ml in a 6-well plate containing THY and incubated at 37°C in a 5% CO_2 atmosphere. The supernatant containing planktonic bacteria was collected 0, 1, 2, or 4 h postinoculation and then centrifuged at 8,000 rpm for 10 min to separate the planktonic cells; the supernatant was further filtered through a 0.45-μm syringe filter. The concentration of H_2O_2 present in each cell-free supernatant was assessed using an Amplex Red hydrogen peroxide/peroxidase assay kit (Invitrogen) following the manufacturer's instructions.

Detection of hydroxyl radicals by spin trapping. A spin-trapping system was utilized to detect the formation of hydroxyl radicals essentially as described previously (38, 51). Briefly, pneumococci were grown in 100 ml of THY broth to an OD_{600} of 0.4 to 0.5. The pellets were harvested and washed twice with Hanks balanced salt solution lacking calcium and magnesium (HBSS) and finally resuspended in 500 μl of HBSS. The reaction mixtures included 200 μl of cell suspension, 100 μM diethylenetriaminepentaacetic acid (DETAPAC), 10 mM 4-POBN, 170 mM ethanol, and HBSS for a final volume of 1 ml. The reaction mixture was incubated for 10 min at room temperature and immediately transferred to a quartz capillary tube (2-mm outer diameter), and X-band electron paramagnetic resonance (EPR) spectra were acquired under the following conditions: microwave frequency, 9.346 GHz; microwave power, 10 mW; modulation amplitude, 0.2 mT; modulation frequency, 100 kHz; temperature, 295 K; the spectra represent an average of 92 scans minus a medium baseline (224 scans).

***S. aureus* strain sequence and phylogeny.** In brief, Nextera random shotgun libraries were prepared, and 300-bp paired-end reads were sequenced to >20 to 100× coverage. Sequence types were ascribed based on BLASTN against the BIGSdb database (52, 53). The phylogeny was created using Parsnp (54) based on mapping to the Newman reference. The tree was midpoint rooted and visualized using iTOL (55).

Statistical analysis. Differences between *S. aureus* strain sensitivities to *S. pneumoniae* were calculated by a Kruskal-Wallis test for overall variability in the collection. The test was performed for all strains with or without the two most sensitive strains (NRS408 and NRS170). All other statistical analysis was performed using a two-tailed Student *t* test and the software SigmaPlot version 14.0.

Accession number(s). The data were deposited in NCBI BioProject under accession no. PRJNA289526 as part of a larger study that will be described in more detail elsewhere.

SUPPLEMENTAL MATERIAL

Supplemental material for this article may be found at https://doi.org/10.1128/JB.00474-19.

SUPPLEMENTAL FILE 1, PDF file, 0.3 MB.

ACKNOWLEDGMENTS

This study was supported by a grant from the National Institutes of Health (NIH) (R21AI112768-01A1 and 1R21AI144571-01 to J.E.V.). The confocal studies were in part supported by funds from the Integrated Cellular Imaging (ICI) pediatric core and the Emory+Children's Pediatric Research Center to J.E.V. Funds from the Raymond F. Schinazi International Exchange Program (SIEP), a faculty exchange program between the Read laboratory at Emory University and the Hadassah Medical Organization to promote collaborative research and education, supported O.G. EPR spectroscopy was supported by NIH grants R01DK054514 and NIH RR17767 (to K.W.). U.A.A.-Z. thanks CONACyT for mobility scholarship 291250.

The content is solely our responsibility and does not necessarily represent the official views of the National Institutes of Health.

We thank Faidad Khan (Emory University) for his assistance in some experiments and Marc Lipsitch (Harvard T. H. Chan School of Public Health) for providing us with TIGR4 and Pn20 hydrogen peroxide-deficient mutants.

REFERENCES

1. Regev-Yochay G, Dagan R, Raz M, Carmeli Y, Shainberg B, Derazne E, Rahav G, Rubinstein E. 2004. Association between carriage of Streptococcus pneumoniae, and Staphylococcus aureus in children. JAMA 292:716–720. https://doi.org/10.1001/jama.292.6.716.
2. Bakaletz LO. 2007. Bacterial biofilms in otitis media: evidence and relevance. Pediatr Infect Dis J 26:S17–S19. https://doi.org/10.1097/INF.0b013e318154b273.
3. Dunne EM, Smith-Vaughan HC, Robins-Browne RM, Mulholland EK, Satzke C. 2013. Nasopharyngeal microbial interactions in the era of pneumococcal conjugate vaccination. Vaccine 31:2333–2342. https://doi.org/10.1016/j.vaccine.2013.03.024.
4. Shak JR, Cremers AJ, Gritzfeld JF, de Jonge MI, Hermans PW, Vidal JE, Klugman KP, Gordon SB. 2014. Impact of experimental human pneumococcal carriage on nasopharyngeal bacterial densities in healthy adults. PLoS One 9:e98829. https://doi.org/10.1371/journal.pone.0098829.
5. Shak JR, Vidal JE, Klugman KP. 2013. Influence of bacterial interactions on pneumococcal colonization of the nasopharynx. Trends Microbiol 21:129–135. https://doi.org/10.1016/j.tim.2012.11.005.

6. Vidal JE, Howery KE, Ludewick HP, Nava P, Klugman KP. 2013. Quorum-sensing systems LuxS/Autoinducer 2 and Com regulate Streptococcus pneumoniae biofilms in a bioreactor with living cultures of human respiratory cells. Infect Immun 81:1341–1353. https://doi.org/10.1128/IAI.01096-12.
7. Chien YW, Vidal JE, Grijalva CG, Bozio C, Edwards KM, Williams JV, Griffin MR, Verastegui H, Hartinger SM, Gil AI, Lanata CF, Klugman KP. 2013. Density interactions among Streptococcus pneumoniae, Haemophilus influenzae and Staphylococcus aureus in the nasopharynx of young Peruvian children. Pediatr Infect Dis J 32:72–77. https://doi.org/10.1097/INF.0b013e318270d850.
8. Bogaert D, van Belkum A, Sluijter M, Luijendijk A, de Groot R, Rumke HC, Verbrugh HA, Hermans PW. 2004. Colonisation by Streptococcus pneumoniae and Staphylococcus aureus in healthy children. Lancet 363:1871–1872. https://doi.org/10.1016/S0140-6736(04)16357-5.
9. Chao Y, Marks LR, Pettigrew MM, Hakansson AP. 2014. Streptococcus pneumoniae biofilm formation and dispersion during colonization and disease. Front Cell Infect Microbiol 4:194. https://doi.org/10.3389/fcimb.2014.00194.
10. Gritzfeld JF, Cremers AJ, Ferwerda G, Ferreira DM, Kadioglu A, Hermans PW, Gordon SB. 2014. Density and duration of experimental human pneumococcal carriage. Clin Microbiol Infect 20:O1145–1151. https://doi.org/10.1111/1469-0691.12752.
11. Yarwood JM, Bartels DJ, Volper EM, Greenberg EP. 2004. Quorum sensing in Staphylococcus aureus biofilms. J Bacteriol 186:1838–1850. https://doi.org/10.1128/jb.186.6.1838-1850.2004.
12. Shenoy AT, Brissac T, Gilley RP, Kumar N, Wang Y, Gonzalez-Juarbe N, Hinkle WS, Daugherty SC, Shetty AC, Ott S, Tallon LJ, Deshane J, Tettelin H, Orihuela CJ. 2017. Streptococcus pneumoniae in the heart subvert the host response through biofilm-mediated resident macrophage killing. PLoS Pathog 13:e1006582. https://doi.org/10.1371/journal.ppat.1006582.
13. Brissac T, Shenoy AT, Patterson LA, Orihuela CJ. 2018. Cell invasion and pyruvate oxidase derived H2O2 are critical for Streptococcus pneumoniae mediated cardiomyocyte killing. Infect Immun 86:e00569-17. https://doi.org/10.1128/IAI.00569-17.
14. Regev-Yochay G, Malley R, Rubinstein E, Raz M, Dagan R, Lipsitch M. 2008. In vitro bactericidal activity of Streptococcus pneumoniae and bactericidal susceptibility of Staphylococcus aureus strains isolated from cocolonized versus noncocolonized children. J Clin Microbiol 46:747–749. https://doi.org/10.1128/JCM.01781-07.
15. Bhattacharya M, Wozniak DJ, Stoodley P, Hall-Stoodley L. 2015. Prevention and treatment of Staphylococcus aureus biofilms. Expert Rev Anti-Infect Ther 13:1499–1516. https://doi.org/10.1586/14787210.2015.1100533.
16. Chochua S, D'Acremont V, Hanke C, Alfa D, Shak J, Kilowoko M, Kyungu E, Kaiser L, Genton B, Klugman KP, Vidal JE. 2016. Increased nasopharyngeal density and concurrent carriage of Streptococcus pneumoniae, Haemophilus influenzae, and Moraxella catarrhalis are associated with pneumonia in febrile children. PLoS One 11:e0167725. https://doi.org/10.1371/journal.pone.0167725.
17. Morgan HJ, Avery OT. 1924. Growth-inhibitory substances in pneumococcus cultures. J Exp Med 39:335–346. https://doi.org/10.1084/jem.39.3.335.
18. Avery OT, Morgan HJ. 1924. The occurrence of peroxide in cultures of Pneumococcus. J Exp Med 39:275–287. https://doi.org/10.1084/jem.39.2.275.
19. Pericone CD, Overweg K, Hermans PW, Weiser JN. 2000. Inhibitory and bactericidal effects of hydrogen peroxide production by Streptococcus pneumoniae on other inhabitants of the upper respiratory tract. Infect Immun 68:3990–3997. https://doi.org/10.1128/IAI.68.7.3990-3997.2000.
20. Regev-Yochay G, Trzcinski K, Thompson CM, Malley R, Lipsitch M. 2006. Interference between Streptococcus pneumoniae and Staphylococcus aureus: in vitro hydrogen peroxide-mediated killing by Streptococcus pneumoniae. J Bacteriol 188:4996–5001. https://doi.org/10.1128/JB.00317-06.
21. Pericone CD, Bae D, Shchepetov M, McCool T, Weiser JN. 2002. Short-sequence tandem and nontandem DNA repeats and endogenous hydrogen peroxide production contribute to genetic instability of Streptococcus pneumoniae. J Bacteriol 184:4392–4399. https://doi.org/10.1128/jb.184.16.4392-4399.2002.
22. Yesilkaya H, Andisi VF, Andrew PW, Bijlsma JJ. 2013. Streptococcus pneumoniae and reactive oxygen species: an unusual approach to living with radicals. Trends Microbiol 21:187–195. https://doi.org/10.1016/j.tim.2013.01.004.
23. Khan F, Wu X, Matzkin GL, Khan MA, Sakai F, Vidal JE. 2016. Streptococcus pneumoniae eradicates preformed Staphylococcus aureus biofilms through a mechanism requiring physical contact. Front Cell Infect Microbiol 6:104. https://doi.org/10.3389/fcimb.2016.00104.
24. Lisher JP, Tsui HT, Ramos-Montanez S, Hentchel KL, Martin JE, Trinidad JC, Winkler ME, Giedroc DP. 2017. Biological and chemical adaptation to endogenous hydrogen peroxide production in Streptococcus pneumoniae D39. mSphere 2:e00291-16. https://doi.org/10.1128/mSphere.00291-16.
25. Ramos-Montanez S, Tsui HC, Wayne KJ, Morris JL, Peters LE, Zhang F, Kazmierczak KM, Sham LT, Winkler ME. 2008. Polymorphism and regulation of the spxB (pyruvate oxidase) virulence factor gene by a CBS-HotDog domain protein (SpxR) in serotype 2 Streptococcus pneumoniae. Mol Microbiol 67:729–746. https://doi.org/10.1111/j.1365-2958.2007.06082.x.
26. Taniai H, Iida K, Seki M, Saito M, Shiota S, Nakayama H, Yoshida S. 2008. Concerted action of lactate oxidase and pyruvate oxidase in aerobic growth of Streptococcus pneumoniae: role of lactate as an energy source. J Bacteriol 190:3572–3579. https://doi.org/10.1128/JB.01882-07.
27. Park B, Nizet V, Liu GY. 2008. Role of Staphylococcus aureus catalase in niche competition against Streptococcus pneumoniae. J Bacteriol 190:2275–2278. https://doi.org/10.1128/JB.00006-08.
28. Echlin H, Frank MW, Iverson A, Chang TC, Johnson MD, Rock CO, Rosch JW. 2016. Pyruvate oxidase as a critical link between metabolism and capsule biosynthesis in Streptococcus pneumoniae. PLoS Pathog 12:e1005951. https://doi.org/10.1371/journal.ppat.1005951.
29. Bryant JC, Dabbs RC, Oswalt KL, Brown LR, Rosch JW, Seo KS, Donaldson JR, McDaniel LS, Thornton JA. 2016. Pyruvate oxidase of Streptococcus pneumoniae contributes to pneumolysin release. BMC Microbiol 16:271. https://doi.org/10.1186/s12866-016-0881-6.
30. Margolis E. 2009. Hydrogen peroxide-mediated interference competition by Streptococcus pneumoniae has no significant effect on Staphylococcus aureus nasal colonization of neonatal rats. J Bacteriol 191:571–575. https://doi.org/10.1128/JB.00950-08.
31. Margolis E, Yates A, Levin BR. 2010. The ecology of nasal colonization of Streptococcus pneumoniae, Haemophilus influenzae and Staphylococcus aureus: the role of competition and interactions with host's immune response. BMC Microbiol 10:59. https://doi.org/10.1186/1471-2180-10-59.
32. Reiss-Mandel A, Regev-Yochay G. 2016. Staphylococcus aureus and Streptococcus pneumoniae interaction and response to pneumococcal vaccination: myth or reality? Hum Vaccin Immunother 12:351–357. https://doi.org/10.1080/21645515.2015.1081321.
33. Hoepelman IM, Bezemer WA, Vandenbroucke-Grauls CM, Marx JJ, Verhoef J. 1990. Bacterial iron enhances oxygen radical-mediated killing of Staphylococcus aureus by phagocytes. Infect Immun 58:26–31.
34. Repine JE, Fox RB, Berger EM. 1981. Hydrogen peroxide kills Staphylococcus aureus by reacting with staphylococcal iron to form hydroxyl radical. J Biol Chem 256:7094–7096.
35. Imlay JA, Chin SM, Linn S. 1988. Toxic DNA damage by hydrogen peroxide through the Fenton reaction in vivo and in vitro. Science 240:640–642. https://doi.org/10.1126/science.2834821.
36. Quillin SJ, Hockenberry AJ, Jewett MC, Seifert HS. 2018. Neisseria gonorrhoeae exposed to sublethal levels of hydrogen peroxide mounts a complex transcriptional response. mSystems 3:e00156-18. https://doi.org/10.1128/mSystems.00156-18.
37. Wong SM, Alugupalli KR, Ram S, Akerley BJ. 2007. The ArcA regulon and oxidative stress resistance in Haemophilus influenzae. Mol Microbiol 64:1375–1390. https://doi.org/10.1111/j.1365-2958.2007.05747.x.
38. Pericone CD, Park S, Imlay JA, Weiser JN. 2003. Factors contributing to hydrogen peroxide resistance in Streptococcus pneumoniae include pyruvate oxidase (SpxB) and avoidance of the toxic effects of the Fenton reaction. J Bacteriol 185:6815–6825. https://doi.org/10.1128/jb.185.23.6815-6825.2003.
39. Imlay JA. 2008. Cellular defenses against superoxide and hydrogen peroxide. Annu Rev Biochem 77:755–776. https://doi.org/10.1146/annurev.biochem.77.061606.161055.
40. Gonzalez-Flecha B, Demple B. 1995. Metabolic sources of hydrogen peroxide in aerobically growing Escherichia coli. J Biol Chem 270:13681–13687. https://doi.org/10.1074/jbc.270.23.13681.
41. Selva L, Viana D, Regev-Yochay G, Trzcinski K, Corpa JM, Lasa I, Novick RP, Penadés JR. 2009. Killing niche competitors by remote-control bac-

teriophage induction. Proc Natl Acad Sci U S A 106:1234–1238. https://doi.org/10.1073/pnas.0809600106.
42. Imlay JA, Linn S. 1988. DNA damage and oxygen radical toxicity. Science 240:1302–1309. https://doi.org/10.1126/science.3287616.
43. Tettelin H, Nelson KE, Paulsen IT, Eisen JA, Read TD, Peterson S, Heidelberg J, DeBoy RT, Haft DH, Dodson RJ, Durkin AS, Gwinn M, Kolonay JF, Nelson WC, Peterson JD, Umayam LA, White O, Salzberg SL, Lewis MR, Radune D, Holtzapple E, Khouri H, Wolf AM, Utterback TR, Hansen CL, McDonald LA, Feldblyum TV, Angiuoli S, Dickinson T, Hickey EK, Holt IE, Loftus BJ, Yang F, Smith HO, Venter JC, Dougherty BA, Morrison DA, Hollingshead SK, Fraser CM. 2001. Complete genome sequence of a virulent isolate of *Streptococcus pneumoniae*. Science 293:498–506. https://doi.org/10.1126/science.1061217.
44. Vidal JE, Ludewick HP, Kunkel RM, Zahner D, Klugman KP. 2011. The LuxS-dependent quorum-sensing system regulates early biofilm formation by Streptococcus pneumoniae strain D39. Infect Immun 79:4050–4060. https://doi.org/10.1128/IAI.05186-11.
45. Wu X, Jacobs NT, Bozio C, Palm P, Lattar SM, Hanke CR, Watson DM, Sakai F, Levin BR, Klugman KP, Vidal JE. 2017. Competitive dominance within biofilm consortia regulates the relative distribution of pneumococcal nasopharyngeal density. Appl Environ Microbiol 83:e00953-17. https://doi.org/10.1128/AEM.00953-17.
46. Carvalho MDGS, Tondella ML, McCaustland K, Weidlich L, McGee L, Mayer LW, Steigerwalt A, Whaley M, Facklam RR, Fields B, Carlone G, Ades EW, Dagan R, Sampson JS. 2007. Evaluation and improvement of real-time PCR assays targeting *lytA*, *ply*, and *psaA* genes for detection of pneumococcal DNA. J Clin Microbiol 45:2460–2466. https://doi.org/10.1128/JCM.02498-06.
47. Kilic A, Muldrew KL, Tang YW, Basustaoglu AC. 2010. Triplex real-time polymerase chain reaction assay for simultaneous detection of Staphylococcus aureus and coagulase-negative staphylococci and determination of methicillin resistance directly from positive blood culture bottles. Diagn Microbiol Infect Dis 66:349–355. https://doi.org/10.1016/j.diagmicrobio.2009.11.010.
48. Higuchi R, Krummel B, Saiki RK. 1988. A general method of in vitro preparation and specific mutagenesis of DNA fragments: study of protein and DNA interactions. Nucleic Acids Res 16:7351–7367. https://doi.org/10.1093/nar/16.15.7351.
49. Horton RM, Hunt HD, Ho SN, Pullen JK, Pease LR. 1989. Engineering hybrid genes without the use of restriction enzymes: gene splicing by overlap extension. Gene 77:61–68. https://doi.org/10.1016/0378-1119(89)90359-4.
50. Havarstein LS, Coomaraswamy G, Morrison DA. 1995. An unmodified heptadecapeptide pheromone induces competence for genetic transformation in *Streptococcus pneumoniae*. Proc Natl Acad Sci U S A 92:11140–11144. https://doi.org/10.1073/pnas.92.24.11140.
51. Park S, You X, Imlay JA. 2005. Substantial DNA damage from submicromolar intracellular hydrogen peroxide detected in Hpx- mutants of Escherichia coli. Proc Natl Acad Sci U S A 102:9317–9322. https://doi.org/10.1073/pnas.0502051102.
52. Jolley KA, Maiden MC. 2010. BIGSdb: scalable analysis of bacterial genome variation at the population level. BMC Bioinformatics 11:595–510. https://doi.org/10.1186/1471-2105-11-595.
53. Petit RA III, Read TD. 2018. Staphylococcus aureus viewed from the perspective of 40,000+ genomes. Peer J 6:e5261. https://doi.org/10.7717/peerj.5261.
54. Treangen TJ, Ondov BD, Koren S, Phillippy AM. 2014. The Harvest suite for rapid core-genome alignment and visualization of thousands of intraspecific microbial genomes. Genome Biol 15:524–510. https://doi.org/10.1186/s13059-014-0524-x.
55. Letunic I, Bork P. 2016. Interactive tree of life (iTOL) v3: an online tool for the display and annotation of phylogenetic and other trees. Nucleic Acids Res 44:W242–W245. https://doi.org/10.1093/nar/gkw290.
56. Boake WC. 1956. Antistaphylocoagulase in experimental staphylococcal infections. J Immunol 76:89–96.
57. Nair D, Memmi G, Hernandez D, Bard J, Beaume M, Gill S, Francois P, Cheung AL. 2011. Whole-genome sequencing of Staphylococcus aureus strain RN4220, a key laboratory strain used in virulence research, identifies mutations that affect not only virulence factors but also the fitness of the strain. J Bacteriol 193:2332–2335. https://doi.org/10.1128/JB.00027-11.